PCCP

Accepted Manuscript

ROYAL SOCIETY OF CHEMISTRY

www.rsc.org/pccp

PCCP

ARTICLE

Molecular Dynamics Modeling of Carbon Dioxide, Water and Natural Organic Matter in Na-Hectorite

Received 00th January 20xx,
Accepted 00th January 20xx

DOI: 10.1039/x0xx00000x

www.rsc.org/

A. Ozgur Yazaydin,*[ab] Geoffrey M. Bowers[c] and R. James Kirkpatrick[d]

Molecular dynamics (MD) modeling of systems containing a Na-exchanged smectite clay (hectorite) and model natural organic matter (NOM) molecules along with pure H_2O, pure CO_2, or a mixture of H_2O and CO_2 provides significant new insight into the molecular scale interactions among silicate surfaces, dissolved cations and organic molecules, H_2O and CO_2 relevant to geological C-sequestration strategies. The simulations for systems containing H_2O show the following results; 1. Na^+ does not bridge between NOM molecules and the clay surface at protonation states comparable to near neutral pH conditions. 2. In systems without CO_2 the NOM molecules retain charge balancing cations and drift away from the silicate surface. 3. In systems containing both H_2O and CO_2, the NOM molecules adopt equilibrium positions at the H_2O-CO_2 interface with the more hydrophilic structural elements facing the H_2O and the more hydrophobic ones facing the CO_2. In systems with only CO_2, NOM and Na^+ ions are pinned to the clay surface with the hydrophilic structural elements of the NOM pointed toward the clay surface. Dynamically, in systems with only CO_2, Na^+ diffusion is nearly eliminated, and in systems with a thin water film on the clay surface diffusion perpendicular the surface is greatly reduced relative to the system with bulk water. Energetically, the results for the systems with only H_2O show that hydration of the net charge neutral Na-NOM molecule outweighs the sum of its Coulombic and dispersive interactions with the net charge-neutral Na-clay particle and the interactions of the water molecules with the hydrophobic structural elements of the NOM. The aggregation of NOM molecules in solution appears to be driven not by Na^+ bridging between the molecules but by hydrophobic interactions between them. In contrast, for the systems with only CO_2 the interaction between the Na-NOM molecules and the CO_2 is outweighed by the interaction of NOM with the clay particle. With both H_2O and CO_2 present, the energetic interactions leading to the hydration of the Na-clay surface and the hydrophilic structural elements of the Na-NOM molecule and the hydrophobic interactions between the CO_2 and the hydrophobic aromatic and aliphatic structural elements of the NOM can both be satisfied, leading to the Na-NOM molecules migrating away from the surface and residing at the H_2O-CO_2 interface. The MD results suggest some alternative explanations for the previously observed ^{23}Na NMR behavior of Na-hectorite at elevated temperatures and CO_2 pressures.

Introduction

The interactions among minerals, aqueous solutions, and organic- and bio-molecules are central to fundamental understanding of global carbon balance; soil biogeochemistry; plant nutrition; processes in sediments, soils, sedimentary rocks, and the oceans; and the transport and fate of heavy metals and radionuclides, anionic, organic, and pharmaceutical contaminants.[1-13] Flocculated natural organic matter (NOM) is also a leading cause of water filtration membrane fouling.[14-16] These interactions have been the focus of a wide range of analytical, experimental, theoretical and computational studies since at least the 1960s.[3, 17-22] The extent of metal-NOM binding with a given substrate varies with the size, composition and conformation of the NOM; the ionic strength and pH of the solution; the chemical properties of the metal; and the metal/NOM compositional ratio.[11, 23, 24] In the natural environment, binding of NOM to the surfaces of silicate minerals is of particular importance to understand colloid formation in natural waters and the chemical behavior in the nanopores of organic rich shales.

Computational modeling has played an important role in understanding the molecular scale interactions of organic- and bio-molecules with silicate mineral surfaces. In early studies, Shevchenko and Bailey[21, 22, 25] used energy minimization and molecular dynamics (MD) methods to study the interaction of model bio-molecules with muscovite mica as a model for clay minerals with and without water molecules present. More recently, Sutton and Sposito[10] undertook detailed molecular dynamics (MD) studies of the interactions of the swelling clay montmorillonite with NOM molecules with Ca^{2+} as the charge balancing cation. The results showed that the protonation

[a] Department of Chemical Engineering, University College London, London, WC1E7JE, United Kingdom. E-mail: ozgur.yazaydin@ucl.ac.uk
[b] Department of Chemistry, Michigan State University, East Lansing, Michigan 48824, United States.
[c] Division of Chemistry, Alfred University, 1 Saxon Drive, Alfred, New York, 14802, United States.
[d] College of Natural Science, Michigan State University, East Lansing, Michigan 48824, United States.

state of the organic molecule plays an important role in controlling the interactions with the mineral surface. For models with protonated carboxylic groups (which typically exhibit pK_a values of 4 - 5), the NOM-mineral surface structure is dominated by hydrophobic interactions that minimize the coordination of the NOM molecule by H_2O (see Sutton and Sposito, 2006,[10] for a detailed discussion). In contrast, in systems with deprotonated NOM carboxylic groups more closely approximating near-neutral pH conditions, partially hydrated Ca^{2+} serves as a bridge between the basal oxygen atoms of the clay surface and the deprotonated oxygen atoms of the NOM carboxylic groups.

Computational molecular modeling has also played an important role in understanding the structure and aggregation of NOM dissolved in aqueous solutions.[10, 13, 18, 21, 22, 25-32] One important result of these studies is that the structural and dynamical interactions between the charge balancing cation and the deprotonated carboxylic groups of NOM molecules depends greatly on the hydration energy of the cation. The results show that Cs^+ prefers to coordinate to the carboxylic groups as solvent separated ion pairs (outer sphere complexes),[32] whereas Na^+, Ca^{2+}, and Mg^{2+} prefer to coordinate to these sites as contact ion pairs.[29, 33] The average residence time for cation coordination to the carboxylic group varies over many orders of magnitude.[29, 33] For Na^+ it is between 0.02 and 0.05 ns, and for Ca^{2+} of the order of 0.5 ns. Mg^{2+} does not undergo any site exchange during 10 ns of MD simulation. Aggregation of the model NOM molecules in solution occurs in the presence of Ca^{2+} but not Na^+ or Mg^{2+}.[29, 33] This result is in agreement with previous experimental observations for NOM fouling of water purification membranes,[14] and is consistent with the bridging between montmorillonite surfaces and deprotonated NOM carboxylic groups observed in the simulations of Sutton and Sposito.[10]

CO_2 is often an important component of geochemical fluids, and its interaction with minerals and naturally occurring organic material is especially important in potential geological carbon sequestration scenarios. Both experimental and computational molecular modeling studies have shown that CO_2 can enter clay interlayers,[26, 34-45] and recent high pressure and temperature nuclear magnetic resonance (NMR) studies have suggested that NOM may enhance this interaction.[35] To our knowledge, the only published computational molecular modeling study of CO_2 in clay-organic systems is an MD study of anhydrous Na montmorillonite with interlayer poly(ethylene glycol) (PEG) and CO_2.[42] These simulations showed that although CO_2 is stable in interlayer galleries without PEG, it prefers to coordinate to the ether oxygen atoms (-C-O-C-) of PEG if it is present. The coordination environment of CO_2 with and without PEG present is similar to that observed in supercritical CO_2 and dry ice, although it is highly disordered compared to the crystal structure. The results also show that direct interactions between Na^+ and the mineral surface are disrupted in the presence of PEG, which can effectively solvate the Na^+, but not in the presence of pure CO_2.

This paper presents the results of a MD modeling study of systems containing a smectite clay (hectorite) and model NOM molecules along with pure H_2O, pure CO_2, or a mixture of H_2O and CO_2. These simulations are directed towards natural geologic situations and focus on understanding the interaction of NOM with the exterior surfaces of the clay particles, since NOM does not commonly occur naturally in clay interlayer galleries. The results provide new insight into the molecular scale interactions among silicate surfaces, dissolved cations and organic molecules, H_2O and CO_2.

Computational Methods

Our simulated hectorite model is based on the structure of Breu et al.[36] with Na^+ replacing Cs^+ as the counter ion and with an octahedral Li^+/Mg^{2+} ratio of 1/5 to reflect the composition of the natural San Bernardino hectorite.[46-48] The full details of the hectorite model can be found in our previous publication.[49]

For the NOM molecular fragment, we used the TNB (Temple–Northeastern–Birmingham) model that is frequently used in MD studies of NOM behavior in aqueous solution.[29, 33, 50-52] This model incorporates three carboxylic groups, three carbonyl groups, two phenolic groups, two amine groups, and four other R–OH alcohol groups. It provides a good structural and compositional analogue of the Suwannee River NOM that is commonly used in experimental studies.[14, 30, 32, 50-52] Carboxylic groups are the most important interaction sites for metal binding in many organic and bio-organic molecules and are expected to be so for cation-NOM interactions.[10, 29-31] To model near-neutral pH conditions, our simulations involve permanently protonated hydroxyl and amine groups with all three carboxylic groups deprotonated at all times. This protonation state gives a net -3 charge, which we balance by initially placing 3 Na^+ cations near the carboxylic groups. The overall formula of the NOM model is, thus, $C_{36}O_{16}N_2H_{37}Na_3$ (Figure 1), but the Na^+ ions are not restricted to remain with the NOM molecule.

Water molecules are represented by the flexible SPC[53] model. For CO_2, a fully flexible model recently developed by Cygan and colleagues for clay simulations were used.[26] The ClayFF[54] and CVFF[55] force fields were used for representing the interactions for hectorite and TNB-NOM, respectively. Lorentz–Bertholet mixing rules were used to evaluate the interactions between unlike atom types.[56]

For our simulations we constructed a 4 layer thick Na-hectorite slab consisting of 448 unit cells in a 14a × 8b × 4c arrangement. The hectorite unit cell was originally triclinic, but in the simulation, the slab was converted to orthorhombic symmetry. This gave rise to a slab with a thickness of 77.221Å (Z direction) and side lengths of 73.361Å and 72.754Å (X and Y directions, respectively). Since our interest is in NOM interaction with exterior surfaces, to reduce computational time, no H_2O or CO_2 were included in the interlayer galleries. In order to simulate a nanopore, we then created a void space above the hectorite slab and placed one or two NOM molecules on one of the hectorite surfaces. This structure is comparable to that used by Greathouse et al.[57] to model nanopores in clay-rich shale systems. In all the simulations the

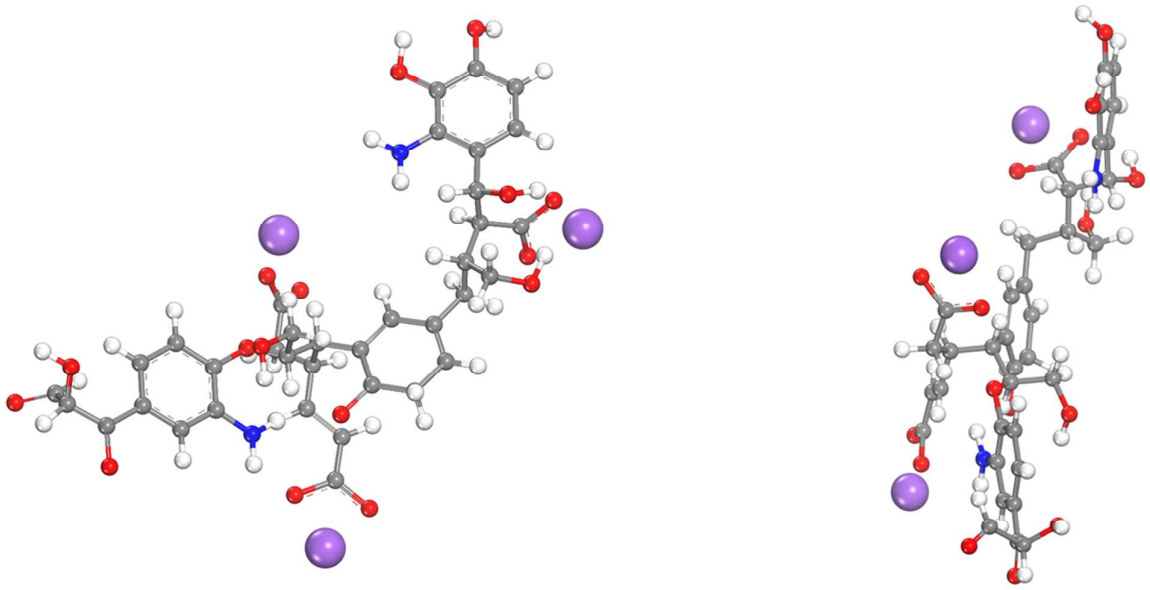

Figure 1. TNB model of NOM shown from two different angles. Oxygen (red), Carbon (gray), Nitrogen (blue), Hydrogen (white), and Na^+ (purple).

NOM molecules were initially oriented with the carboxylic groups facing away from the hectorite surface. For models with two NOM molecules, the centers of the molecules were separated by 20 Å (Figure 2a). The void space was then filled with H_2O and CO_2 molecules in three fluid compositions; pure H_2O (12,000 H_2O molecules), pure CO_2 (4,000 CO_2 molecules), and a 2:1 molar mixture of H_2O and CO_2 (8,000 H_2O and 4,000 CO_2 molecules). In the case of the mixed fluid, water layers were first created on both hectorite surfaces, and the remaining void space was then filled with CO_2 molecules (Figure 2e). Starting with this configuration saved us considerable computational time, because starting from a randomly distributed H_2O and CO_2 mixture would have taken an extremely long equilibration period for the H_2O and CO_2 to separate. Preliminary MD models starting with randomly distributed H_2O and CO_2 molecules showed separation into volumes of nearly pure H_2O and CO_2 comparable to the starting configurations here. All initial positions of H_2O and CO_2 molecules were generated using the PACKMOL package.[58]

All simulations used the DL_POLY4.05 molecular dynamics simulation package[59] and employed 3-dimensional periodic boundary conditions, a 1 fs time step, and a 12 Å cutoff distance. Smoothed particle mesh Ewald summation was used to handle electrostatic interactions. We first performed so-called 'Zero' temperature MD simulations to relax the systems in the NVT ensemble for 0.1ns. This is actually equivalent to a dynamical simulation at low temperature. At each time step the molecules move in the direction of the computed forces, but are not allowed to acquire velocities larger than that corresponding to a temperature of 10 Kelvin. After these short relaxation simulations we performed 2ns of equilibration and 20ns of production simulations at 348.15 K and 130 bars; conditions representative of the conditions in subsurface geological reservoirs. The simulations were performed in the anisotropic NPT ensemble with orthorhombic MD cell constraints. In all simulations the Melchionna et al. modification of the Nosé-Hoover[60, 61] thermostat and barostat were used with 1 ps relaxation times for temperature and pressure control. Radial distribution functions (RDFs) and plots of atomic probability density perpendicular to the clay layers (Z-density) were calculated over the trajectory generated during the 20 ns production run. Mean square displacements (MSDs) for 15 ns were computed using multiple origins through the full production run trajectory.

Results

Z-density plots of Na^+, NOM, H_2O and CO_2 molecules show that the distribution of these species varies greatly with the fluid present and that the structure can also be different with and without NOM near the surface (Figure 3). In simulations with pure CO_2 on the surface without NOM (left surface in Figures 3a and 3b), the Na^+ ions are all closely coordinated to the surface, and the CO_2 has a damped periodic structure of low and high density layers extending about 12 Å into the fluid. The high-density peak near the surface has a shoulder about 1 Å further from the surface than the main peak. On the surface with NOM (right surface in Figures 3a and 3b), the NOM molecules occur in a near-surface region of highly structured CO_2 molecules within about 7 Å of the surface. During the simulations, the NOM molecules reoriented such that their hydrophilic side with deprotonated carboxylic groups is aligned towards the hectorite surface. Na^+ ions coordinated to the carboxylic groups of the NOM remained with the NOM molecules at about 3 Å from the surface (2nd blue peak on the right surface). Analysis of the full trajectory shows that in the simulations with pure CO_2 and two NOM molecules, the two molecules did not aggregate.

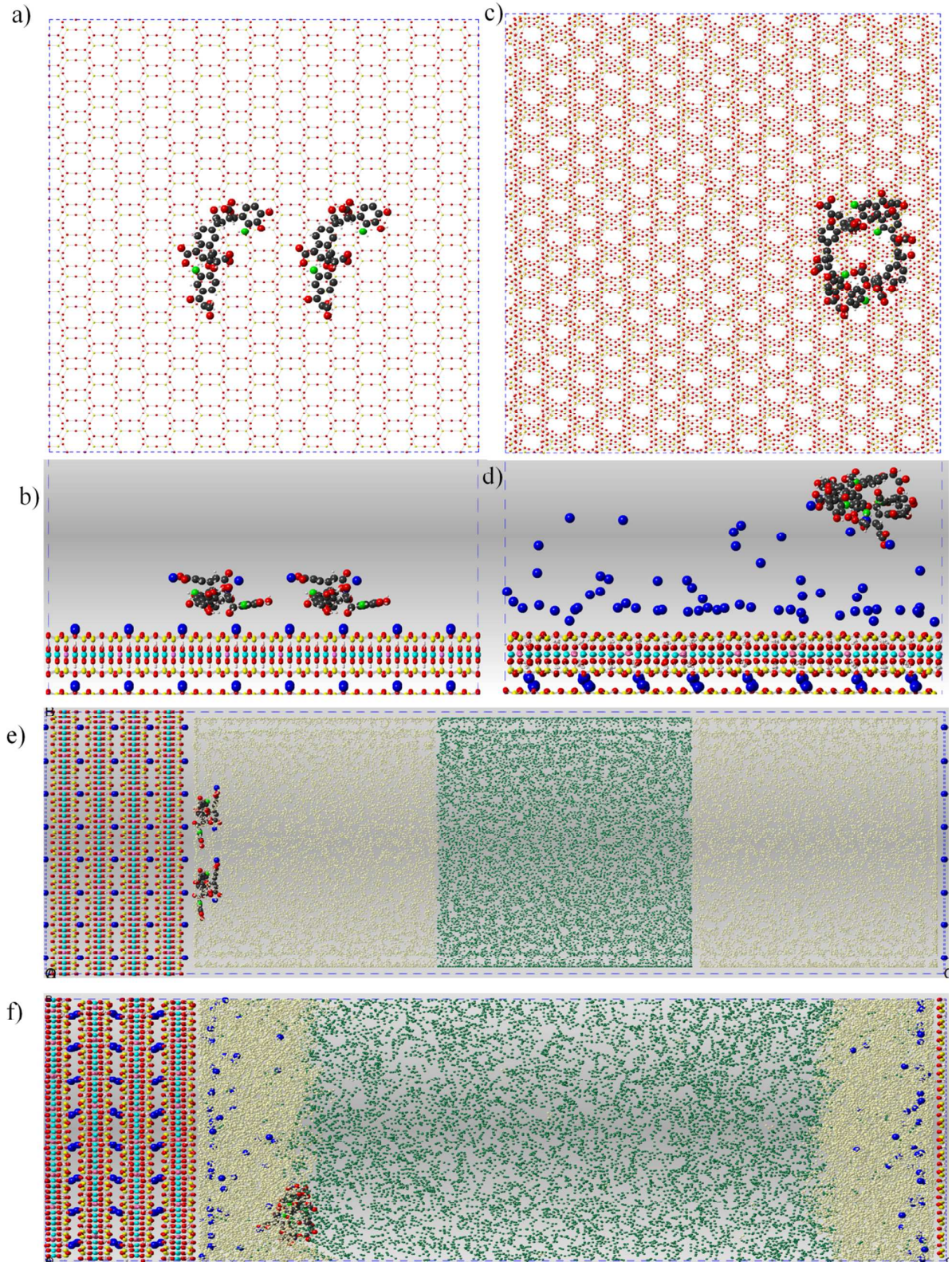

Figure 2. Initial (a and b) and final (c and d) configurations of the system containing 2 NOM molecules and both H_2O and CO_2. Views are presented looking down onto the clay surface (a and c) and from the side (b and d). The full simulation box at the initial (e) and final states (f) viewed from the side are also presented with light yellow and green particles showing the H_2O and CO_2 molecules, respectively. In a ,b, c and d, H_2O and CO_2 molecules are not shown for clarity. In the views looking down onto the clay surface, Na^+, Mg^+ and Li^+ (a and b) are omitted for clarity. Oxygen (red), silicon (yellow), carbon of NOM (black), nitrogen (light green), Na^+ (dark blue), Mg^+ (cyan) and Li^+ (pink)

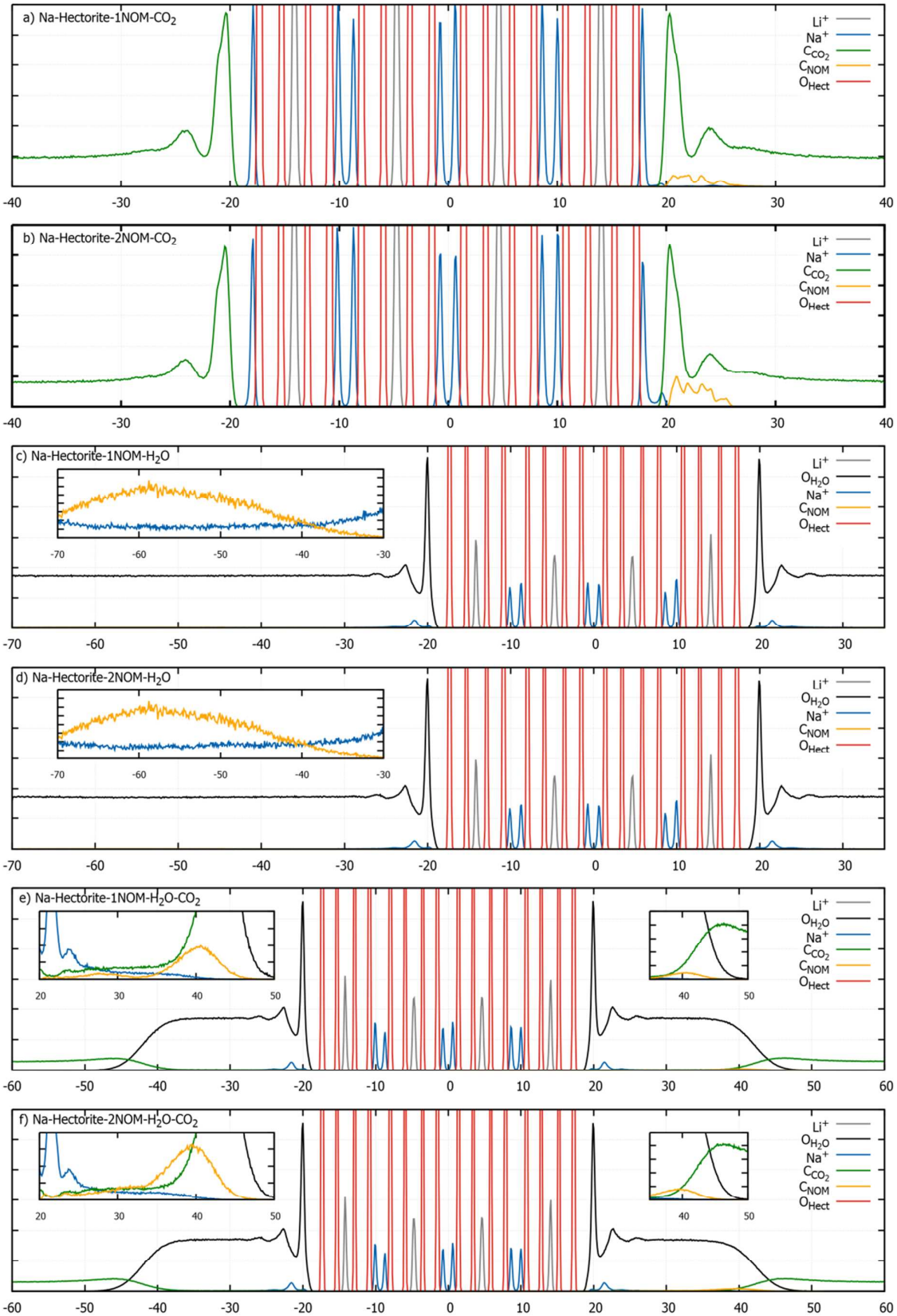

Figure 3. Z-density plots. In all figures the horizontal axis shows position in Å, with 0 at the center of the central hectorite interlayer.

In the simulations with pure water, the NOM molecules diffused away from the surface and remained near the center of the water layer approximately equidistant from the two hectorite surfaces (Figures 3c and 3d). In the simulation with two NOM molecules, the two molecules aggregated. This aggregation appears to be driven by hydrophobic interactions, because no Na^+ ions occur persistently between the two NOM molecules. Importantly, in neither these simulations nor those with pure water, there is no evidence for Na^+ cations bridging the NOM molecules to the surface. As seen in previous MD simulations of Na-smectite systems, most of the Na^+ ions remained near the hectorite surface in outer sphere coordination, and the water shows the typical damped layer structure (see Morrow et al.,[49] for a review). Some of the Na^+ ions, however, diffused away from the surface in association with the NOM molecules to maintain local charge balance.

For the simulations with both H_2O and CO_2 (Figures 3 e and 3f), the CO_2 remains in the center of the fluid volume equidistant from the two hectorite surfaces, and the water and most of the Na^+ occur at the surface with essentially the same structure as with pure H_2O. The H_2O-CO_2 interface is not sharp but has a transition zone about 10 Å thick (see insets on the right hand side in Figures 3e and f). During the simulations a few individual H_2O molecules diffused into the bulk CO_2, and a few individual CO_2 molecules also diffused into the H_2O layer, even reaching the hectorite surface. The NOM molecules diffused away from the surface and remained at the H_2O-CO_2 interface throughout the simulation (Figure 2f). The thickness and structure of the H_2O-CO_2 transition zone is essentially the same with and without NOM present. During these simulations, the NOM molecules flipped their orientation such that their hydrophilic side with deprotonated carboxylic groups was oriented towards the water layer and the hectorite surface (Figure 2b and d). Some of the Na^+ remained associated with the NOM molecules (see insets on the left hand side in Figures 3e and f). In the simulation with two NOM molecules present, the two NOM molecules aggregated early in the simulation and always remained together (Figure 2a and c). As with the pure H_2O system, NOM aggregation appears to be occurring via a hydrophobic mechanism without any Na^+ bridging.

The radial distribution functions (RDFs) between the functional groups of the NOM molecules and the Na^+ ions and H_2O and CO_2 molecules (Figures 4 and 5, and Tables 1 and 2), and the RDFs between the surface Na^+ ions and the oxygen atoms of the clay (Figure 6) provide additional insight into the molecular scale interactions that control the structure observed in the Z-density plots. As expected,[29] the Na^+ ions associated with the NOM molecules are dominantly found in inner sphere coordination with the deprotonated carboxylic groups (Figures 4a and 5a). A few also occur in inner-sphere coordination with the oxygen or nitrogen atoms of the carbonyl, hydroxyl and amine groups at interatomic distances of ~ 2.3-2.8 Å. The running coordination numbers at nearest neighbor distances of less than 3 Å are ~ 0.6 for the carboxylic oxygens but are vanishingly small for the other functional groups (Figures 4d and 5d). These values again demonstrate the importance of metal interactions with carboxylic groups at near neutral pH conditions. RDF peaks in the 4 – 5 Å range represent Na^+ in outer sphere coordination with the various oxygen and nitrogen sites. Well-defined peaks at longer distances are probably the result of the NOM molecular structure rather than specific interactions with individual functional groups.[29] There are some differences in the Na^+ RDFs of the simulations with 1 and 2 NOM molecules, probably reflecting the aggregation of the two NOM molecules in the systems containing H_2O. For instance, with two NOM molecules the carbonyl peak at 2.4 Å is more pronounced, there is a new hydroxyl peak at 2.3 Å, and the amine peak at 2.8 Å present in the case of 1NOM is greatly reduced.

The RDFs and running coordination numbers between the H_2O molecules and the NOM functional groups (Figures 4b and e and 5b and e) reveal that H_2O is coordinated to all functional groups (in particular to the deprotonated carboxylic sites) except the ether oxygen (RDF peak maxima between ~ 2.5 and 3.5 Å). These nearest neighbor distances are typical of hydrogen bonding (H-bonding), as expected for interactions involving amine groups or oxygen atoms of H_2O. The absence of significant coordination to the ether oxygens is probably due to steric hindrance, since the ether oxygen is located almost at the center of the NOM molecule in a predominantly hydrophobic region.

In contrast, the RDFs and running coordination numbers between the CO_2 molecules and the NOM functional groups show that CO_2 coordinates the carbonyl and hydroxyl oxygens and the amine nitrogen but not the carboxylic groups (Figures 4c and f and 5c and f). This is due to the repulsion between the negatively charged oxygens on the CO_2 molecules and carboxylic groups and the orientation of the carboxylic groups towards the water layer on the clay surface and away from the CO_2, as shown by the RDF (blue lines in Figures 4b and c, and 5b and c).

The RDFs and running coordination numbers between the surface Na^+ and the oxygen atoms of the clay (Figures 6a and b) show that in simulations with pure CO_2 the Na^+ ions are strongly associated with the surface. The first peak is at 2.6 Å, which is approximately equal to half the distance between two opposed oxygens in a hexagonal ring of silica tetrahedra on the surface. The corresponding running coordination number of about 6 Å suggests that most of the Na^+ ions are trapped at the centers of the hexagonal rings. The XY projections of the surfaces from the final configurations of these simulations (Figures 6c and d) confirm that the majority of the Na^+ ions are located on these sites, with the remaining few displaced by coordination to the carboxylic groups of the NOM molecule. For the systems with pure H_2O or mixed H_2O and CO_2, the RDFs and running coordination numbers of Na^+ with the surface oxygen atoms are consistent with the Na^+ being in outer sphere coordination as already shown in the Z-density plots.

Analysis of the time dependences of the mean square displacements of the Na^+ ions and their calculated self-diffusivities (Figure 7, Table 3) show significantly different diffusion behavior in the different systems. In the simulations with pure H_2O, the total MSD and the MSDs in the Z-direction

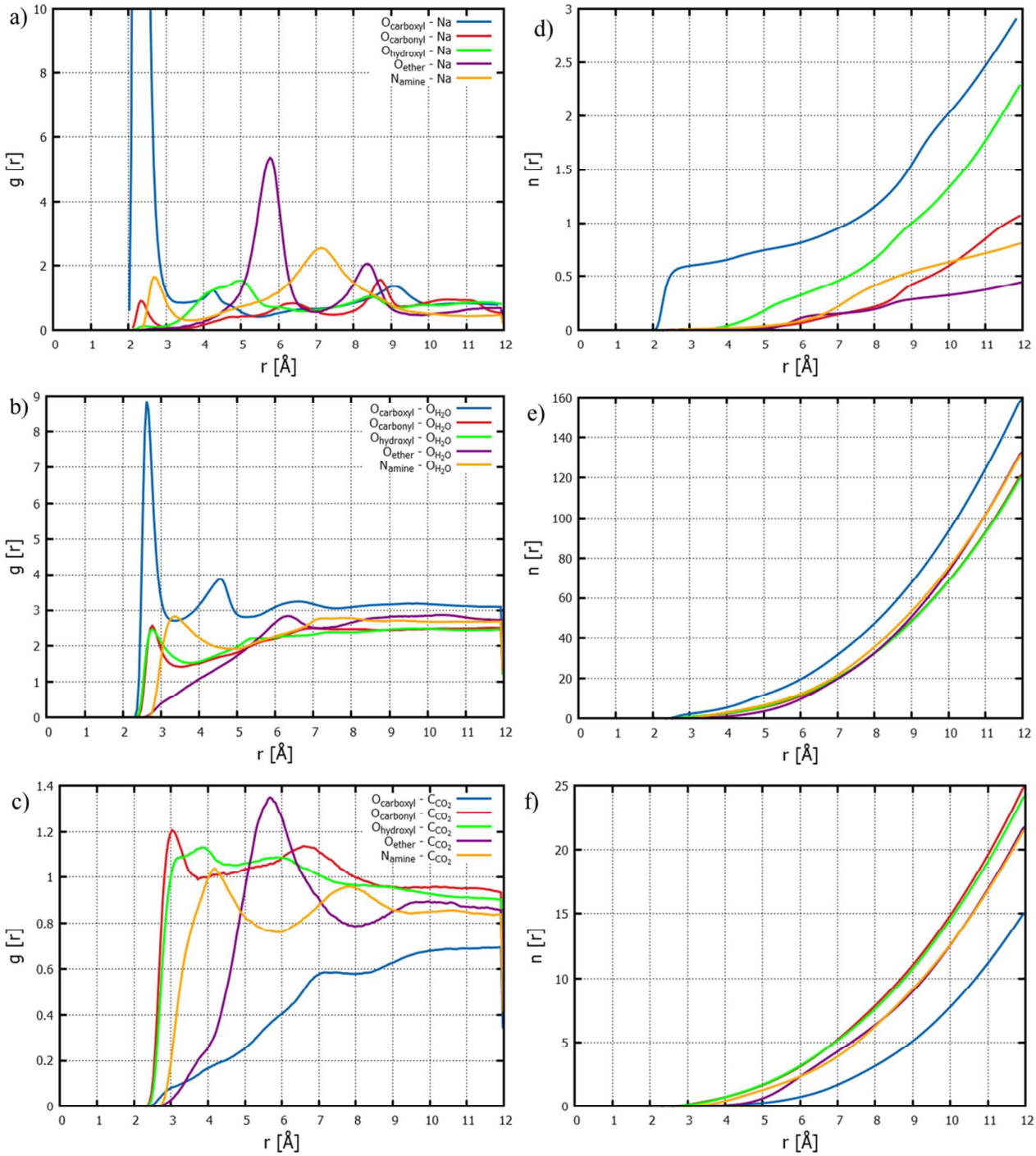

Figure 4. RDF plots between the functional groups of NOM and the Na^+ ions (a), oxygen of H_2O (b) and carbon of CO_2 (c); and the corresponding running coordination numbers (d, e, and f, respectively) in the simulation with 1 NOM molecule containing both H_2O and CO_2.

perpendicular to the clay surface and X and Y directions parallel to it show relatively large, essentially linear increases with time (Figure 7, blue and red lines). The displacement parallel to the interface is significantly greater than that perpendicular to it. This difference is due to the need for the Na^+ to charge balance the negative structural charge of the clay. The diffusion coefficients are of the order of 10^{-5} cm^2/sec, as expected. In the simulations with both H_2O and CO_2 (Figure 7, green and purple lines), the Na^+ displacement in the Z direction (Figure 7d) is greatly reduced due to the relatively thin water layer on the surface. The MSDs in the X and Y directions are only slightly smaller in comparison to the pure

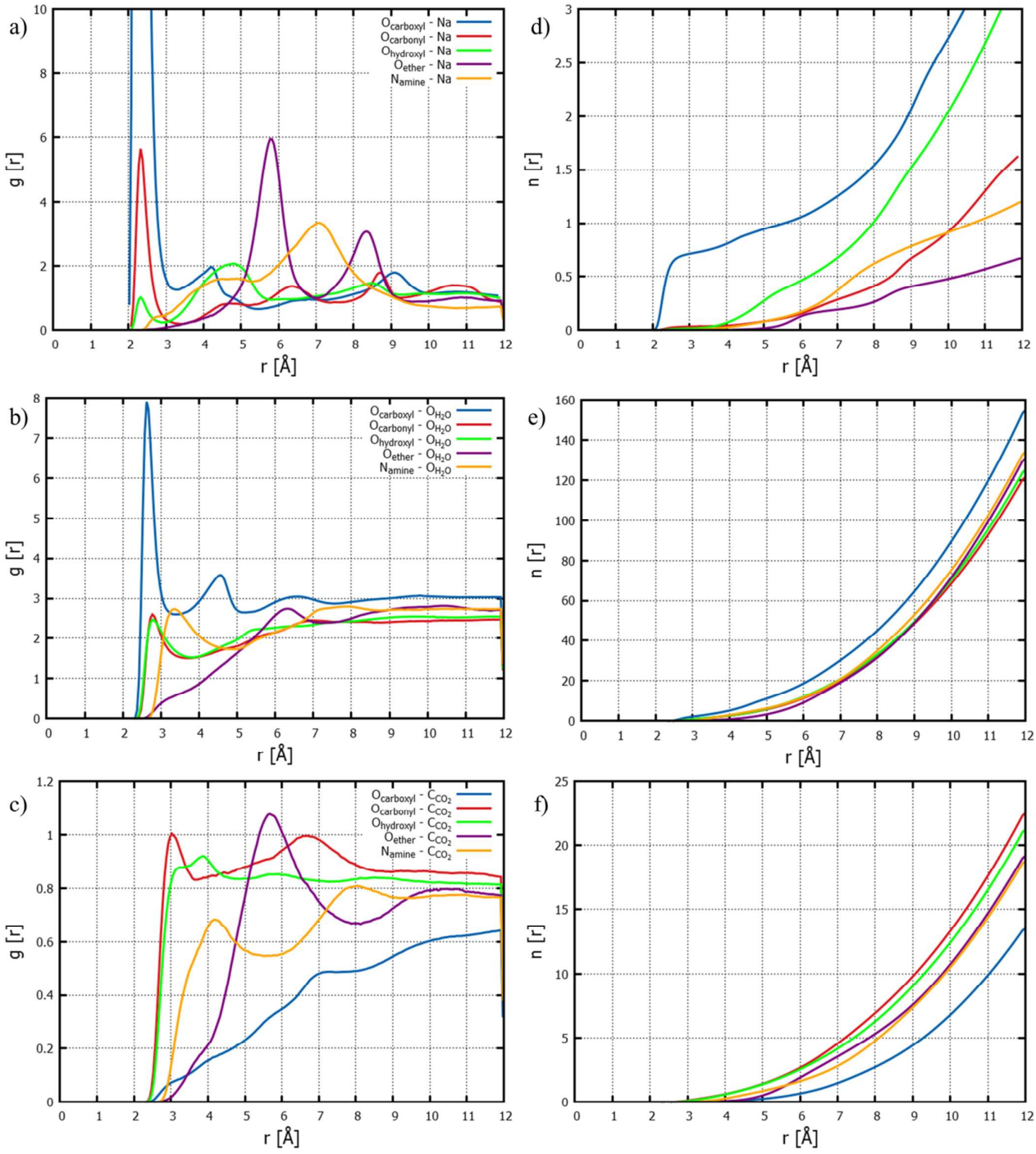

Figure 5. RDF plots between the functional groups of NOM and the Na^+ ions (a), oxygen of H_2O (b) and carbon of CO_2; and the corresponding running coordination numbers (c,d, e, and f, respectively) in simulations with 2 NOM molecules containing both H_2O and CO_2.

H_2O case (Figures 7c and 7d), and the calculated diffusion coefficients are about 10% smaller than those in the pure H_2O system (Table 3). In the simulations with pure CO_2 the surface Na^+ ions show no meaningful long-term MSD, because most of them are trapped on the hexagonal rings due to their insolubility in CO_2.

Discussion and Conclusions

The results presented here provide important new insight into the molecular scale mechanisms by which NOM interacts with mineral surfaces and the influence that supercritical CO_2 under

Table 1. Coordination numbers evaluated at 3 Å from Figures 4.

	Na (Figure 4a)	H_2O (Figure 4b)	CO_2 (Figure 4c)
$O_{carboxyl}$	0.601	2.258	0.009
$O_{carbonyl}$	0.006	0.726	0.146
$O_{hydroxyl}$	0.003	0.765	0.111
O_{ether}	0	0.062	0.002
N_{amine}	0.009	0.182	0.010

Table 2. Coordination numbers evaluated at 3 Å from Figure 5.

	Na (Figure 5a)	H_2O (Figure 5b)	CO_2 (Figure 5c)
$O_{carboxyl}$	0.712	2.076	0.008
$O_{carbonyl}$	0.032	0.758	0.124
$O_{hydroxyl}$	0.145	0.770	0.093
O_{ether}	0	0.064	0.001
N_{amine}	0.003	0.175	0.007

C-sequestration conditions can have on this interaction. One important conclusion is that in situations without CO_2, Na^+ does not play an important role in smectite-NOM binding under near-neutral pH conditions with the carboxylic groups deprotonated. In the simulations here, the NOM molecules and the charge balancing Na^+ ions associated with them drift away from the surface and remain deep within the fluid nanopore for the entire length of the simulation. We note that this could be different from more highly charged clay surfaces, such as illite or those that develop charge in the tetrahedral sheet by Al^{3+} for Si^{4+} substitution. The energetic interactions leading to this configuration for smectites include Coulombic and dispersive (van der Waal's) forces between all the components; hydration of the Na^+ and the clay surface sites; H-bonding involving the water, clay surface and the protonated and deprotonated functional groups on the NOM; and hydrophobic interactions involving the aromatic and aliphatic parts of the NOM molecules. Evaluation of the

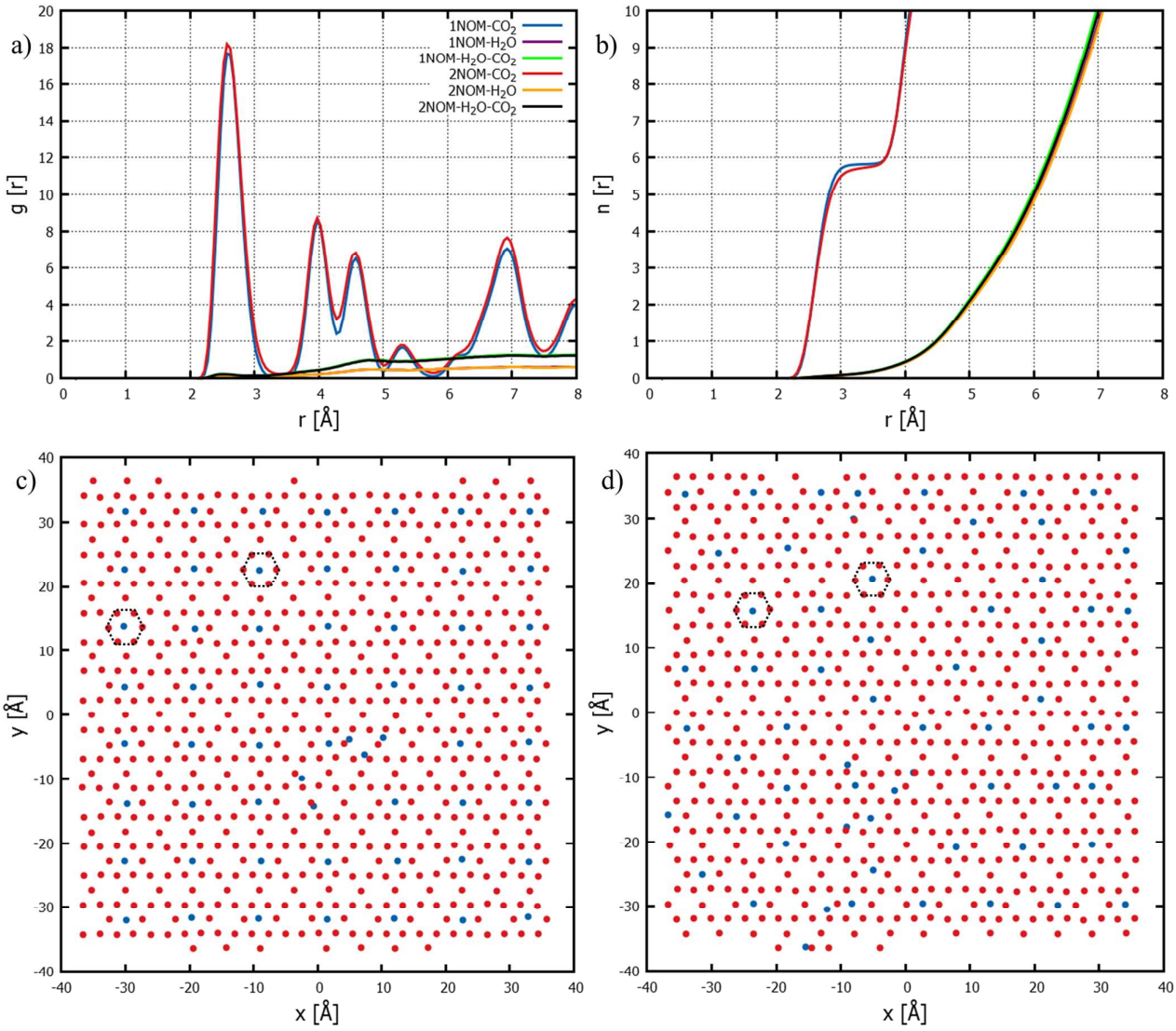

Figure 6. (a) RDFs (b) and running coordination numbers for surface Na^+ and the basal oxygens of hectorite from all simulations; and final x and y coordinates of clay Oxygens (red points) and Na^+ (blue points) from pure CO_2 simulations with (c) 1 NOM molecule and (d) 2 NOM molecules. Most Na^+ ions are trapped at the center of the hexagonal rings on the basal surface of the hectorite (dashed lines).

magnitude of these individual components is beyond the scope of this paper, but it is clear that with only one NOM molecule in the system, the hydration of the net charge neutral NOM molecule with its associated Na^+ ions outweighs the sum of its Coulombic and dispersive interactions with the net charge-neutral Na-clay particle and the interactions of the water molecules with the hydrophobic structural elements of the NOM. The aggregation of the two NOM molecules in the systems containing them appears to be driven not by Na^+ bridging between carboxylic groups but by hydrophobic interactions between the two NOM molecules with their hydrophobic sides oriented towards each other to minimize interaction with the water molecules.

The contrast between the pure H_2O and pure CO_2 systems is striking, with the NOM molecules and their associated Na^+ residing only in the near-surface region when only CO_2 is present. Here, the energetic interaction between the Na-NOM molecules and the CO_2 is outweighed by their interaction with the surface. By analogy with the hydrophobic interaction, one can think of this as a carbonophobic interaction in which the hydrophilic structural elements of the NOM molecules and the hydrophilic Na-smectite surface seek to avoid interaction with the CO_2.

With both H_2O and CO_2 present, the energetic interactions leading to the hydration of the Na-clay surface and the hydrophilic structural elements of the Na-NOM molecule and the hydrophobic interactions between the CO_2 and the hydrophobic/carbonophilic aromatic and aliphatic structural elements of the NOM can both be satisfied, leading to the Na-NOM molecules migrating away from the surface and residing at the H_2O-CO_2 interface. This result also shows that direct interaction of the hydrophobic regions of TNB-NOM molecule outweighs the hydrophobic interactions between it and the CO_2 layer.

Overall, the results here are consistent with the MD modeling results of Iskrenova-Tchoukova et al.[29] and Kalinichev et al.[30] for Na-, Ca-, and Mg-NOM in aqueous solution. Their results and those here show that Na^+ is coordinated to deprotonated carboxylic groups of NOM as inner sphere complexes. Their results over a 10 ns simulation time, however, did not show aggregation of Na-NOM molecules. Our simulations were longer (22 ns) and contained fewer NOM molecules (2 vs. 8) and 4000 or 8000 more water molecules, in addition to the clay particle. Our results are in agreement with experimental data that suggest NOM aggregation depends on the solution ionic strength and

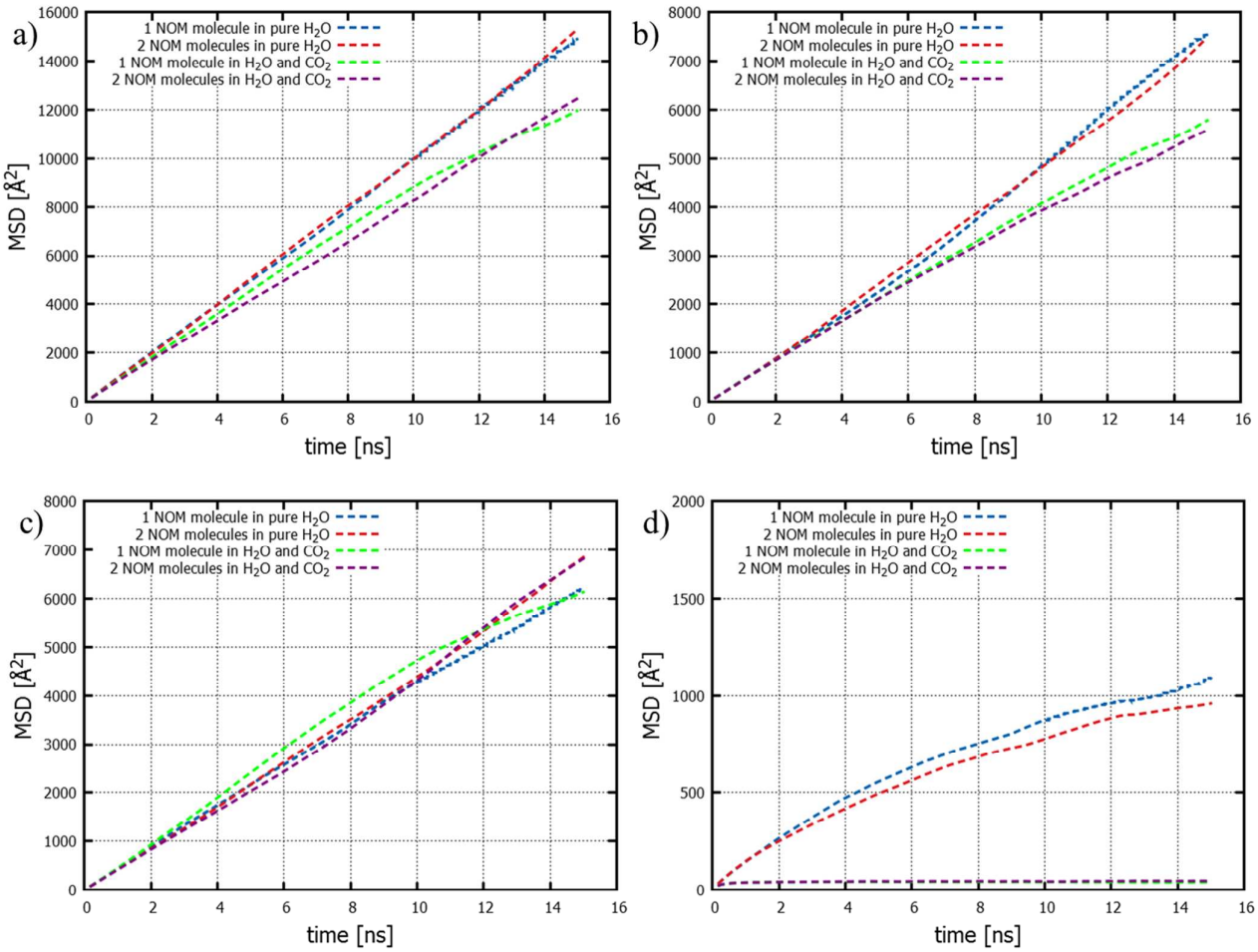

Figure 7. MSD plots of surface Na^+ ions; a) total MSD, and MSDs in the b) X, c) Y and d) Z directions, from Na-Hectorite simulations with pure H_2O and with H_2O and CO_2.

Table 3: Self-diffusion coefficients of surface Na^+ ($cm^2/sec \times 10^5$)

	with 1 NOM molecule	with 2 NOM molecules
Hectorite-H_2O	D_{xyz}=1.66 and D_{xy}=2.32	D_{xyz}=1.68 and D_{xy}=2.36
Hectorite-H_2O-CO_2	D_{xyz}=1.36 and D_{xy}=2.04	D_{xyz}=1.38 and D_{xy}=2.08

activities of both the ions and NOM molecules. The results here are also consistent with those of Sutton and Sposito[10] for NOM in the interlayer galleries of Ca smectite in that they show the importance of hydrophobic interactions and cation coordination to deprotonated carboxylic groups. The Sutton and Sposito,[10] Iskrenova-Tchoukova et al,[29] and Kalinichev et al.[30] results all point to the effectiveness of Ca^{2+} in NOM binding to mineral surface and to itself. Certainly the results here suggest that Na^+ does not play a comparable role.

The results here for the H_2O-CO_2 systems suggest that the presence of CO_2 in C-sequestration reservoirs could lead to mobilization of NOM by detachment from mineral surfaces after CO_2 injection into a water saturated system, although further experiment and modeling with other cations and NOM models with different concentrations of reactive functional groups is necessary to determine if this is a robust conclusion.

The results here also suggest explanations for the previously reported *in situ* NMR observations for Na-hectorite with and without surface- and interlayer-associated humic acid (HA) at a temperature of 50 °C and a CO_2 pressure of 90 bars.[35] The spectroscopic observations were made on Na-hectorite and Na-hectorite-humic acid systems with HA in a fully protonated state that were initially equilibrated at 43% relative humidity (equivalent to a mixture of 1 and 2-layer hydrate layers), although the total system water content after equilibration in $scCO_2$ is unknown. Thus, it is likely that our MD simulations of the pure CO_2 environment and the H_2O/CO_2 mixture represent under-hydrated and over-hydrated end members, suggesting that the MD results can shed significant light on some of the molecular-scale effects observed spectroscopically. For example, the ^{13}C NMR results of Bowers et al.[35] support the idea of stable CO_2 incorporation in the hectorite interlayers, a stronger CO_2 surface association when HA is present, and perhaps greater $scCO_2$ incorporation in the HA-bearing system. These conclusions are consistent with the MD results showing a stable interaction of CO_2 with the clay surface and its preferential association with the hydrophobic regions of the NOM.

Our MD simulations also provide insight into the changes in the ^{23}Na NMR peak positions, line shapes and T_1 relaxation rates reported in Bowers et al.[35] The critical spectroscopic results include an increase in the ^{23}Na signal intensity when $scCO_2$ is present with and without HA, a shift to a more positive peak maximum when $scCO_2$ is added to the HA system, and an increase in the ^{23}Na T_1 relaxation rate (decrease in the T_1 value) for two different observed T_1 environments when $scCO_2$ is present with and without HA. Bowers et al.[35] suggested that these changes are attributable to an increased rate of molecular motion when $scCO_2$ is introduced. This increase is expected to cause a reduced time-averaged quadrupolar interaction for the ^{23}Na sites leading to the signal intensity and position changes. It may also increase intensity of the power spectrum of fluctuations in the electric field gradient at the Na^+ site at the ^{23}Na Larmor frequency, leading to increased T_1 relaxation rates. However, the MD results here suggest that neither NOM nor CO_2 lead to substantial changes in the ^{23}Na diffusion rate or the residence time in hydrated, proximity-restricted environments. These results do not rule out the dynamical explanation offered in Bowers et al.[35] given the differences between the simulations and experimental samples, but they do suggest alternative explanations. For example, the MD results suggest that in the absence of H_2O, CO_2 forces Na^+ tightly onto the surface at the centers of the ditrigonal cavities. This environment would have a different symmetry than the octahedral, hydrated Na^+ coordination environment, resulting in a different quadrupolar coupling constant and potentially explaining the increased signal intensity and change in the position of the peak maximum. Such strong surface associations would also increase the intensity of the dynamical power spectrum at the Larmor frequency, causing the observed increase in T_1 relaxation rate. This hypothesis can be tested using experimental ^{19}F NMR, since the chemical shift of the ^{19}F nuclei found at the base of many ditrigonal cavities in the San Bernardino hectorite is sensitive to cation penetration of the cavity.[62]

The MD results also suggest the possibility that if $scCO_2$ incorporation leads to loss of H_2O prior to NMR data acquisition, the only surviving H_2O in the system could be in the hydration shells of the Na^+ ions due to its carbonophobic nature. This could cause, for instance, Na^+ to occupy inner-sphere coordination sites that would have different electric field gradients and dynamical power spectra than outer-sphere sites. Even if the Na^+ retained a fully hydrated outer sphere coordination, the time averaged electric field gradient and dynamical power spectrum could be affected if reorientation of the hydration shell and exchange of water molecules between it and the extended hydration environment change.

Acknowledgements

The research described in this paper was supported by the United States Department of Energy, Office of Science, Office of Basic Energy Science under award numbers DE-FG02-08ER15929 (R.J.K, P.I.; A.O.Y., co-P.I.) and DE-FG02-10ER16128 (G.M.B., P.I.). We gratefully acknowledge many conversations with Dr. Andrey G. Kalinichev concerning MD modeling of clay and NOM systems.

References

1 A. Kirishima, K. Tanaka, Y. Niibori and O. Tochiyama, *Radiochim. Acta*, 2002, **90**, 555.
2 S. S. Lee, K. L. Nagy, C. Park and P. Fenter, *Environ. Sci. Technol.*, 2011, **45**, 9574-9581.
3 J. A. Leenheer, *Ann. Environ. Sci.*, 2009, **3**, 1-130.
4 A. Piccolo, *Soil Sci.*, 2001, **166**, 810-832.
5 A. Piccolo, *Adv. Agron.*, 2002, **75**, 57-134.
6 H.-R. Schulten and M. Schnitzer, *Soil Sci.*, 1997, **162**, 115-130.

7 G. Sposito, *The surface chemistry of soils*, Oxford University Press, 1984.
8 F. J. Stevenson, *Humus chemistry: genesis, composition, reactions*, John Wiley & Sons, 1994.
9 R. Sutton and G. Sposito, *Environ. Sci. Technol.*, 2005, **39**, 9009-9015.
10 R. Sutton and G. Sposito, *Geochim. Cosmochim. Acta*, 2006, **70**, 3566-3581.
11 E. Tipping, *Cation binding by humic substances*, Cambridge University Press, 2002.
12 R. L. Wershaw, *Evaluation of conceptual models of natural organic matter (humus) from a consideration of the chemical and biochemical processes of humification*, U.S. Geological Survey Scientific Investigations Report 2004-5121, Reston, VA, 2004.
13 R. Sutton, G. Sposito, M. S. Diallo and H. R. Schulten, *Environ. Toxicol. Chem.*, 2005, **24**, 1902-1911.
14 W.-Y. Ahn, A. G. Kalinichev and M. M. Clark, *J. Membr. Sci.*, 2008, **309**, 128-140.
15 S. Hong and M. Elimelech, *J. Membr. Sci.*, 1997, **132**, 159-181.
16 A. Schäfer, A. G. Fane and T. Waite, *Desalination*, 1998, **118**, 109-122.
17 P. M. Bertsch and J. C. Seaman, *Proc. Natl. Acad. Sci. Proc Natl Acad Sci*, 1999, **96**, 3350-3357.
18 B. Chen, J. R. G. Evans, H. C. Greenwell, P. Boulet, P. V. Coveney, A. A. Bowden and A. Whiting, *Chem. Soc. Rev.*, 2008, **37**, 568-594.
19 M. J. Dudas and S. Pawluk, *Geoderma*, 1969, **3**, 5-17.
20 H. Kodama and M. Schnitzer, *Can. J. Soil Sci.*, 1971, **51**, 509-512.
21. S. M. Shevchenko and G. W. Bailey, *THEOCHEM*, 1998, **422**, 259-270.
22 S. M. Shevchenko and G. W. Bailey, *Supramol. Sci.*, 1998, **5**, 143-157.
23 J. Buffle, *Complexation reactions in aquatic systems. An analytical approach*, Ellis Horwood Ltd., Chichester, 1988.
24 J. D. Ritchie and E. M. Perdue, *Geochim. Cosmochim. Acta*, 2003, **67**, 85-96.
25 S. M. Shevchenko, G. W. Bailey and L. G. Akim, *THEOCHEM*, 1999, **460**, 179-190.
26 R. T. Cygan, V. N. Romanov and E. M. Myshakin, *J. Phys. Chem. C*, 2012, **116**, 13079-13091.
27 Y.-T. Fu and H. Heinz, *Philos. Mag.*, 2010, **90**, 2415-2424.
28 J. Greathouse, K. Johnson and H. Greenwell, *Minerals*, 2014, **4**, 519-540.
29 E. Iskrenova-Tchoukova, A. G. Kalinichev and R. J. Kirkpatrick, *Langmuir*, 2010, **26**, 15909-15919.
30 A. G. Kalinichev and R. J. Kirkpatrick, *Eur. J. Soil Sci.*, 2007, **58**, 909-917.
31 A. G. Kalinichev, *Pure Appl. Chem.*, 2012, **85**, 149.
32 X. Xu, A. G. Kalinichev and R. James Kirkpatrick, *Geochim. Cosmochim. Acta*, 2006, **70**, 4319-4331.
33 A. G. Kalinichev, E. Iskrenova-Tchoukova, W.-Y. Ahn, M. M. Clark and R. J. Kirkpatrick, *Geoderma*, 2011, **169**, 27-32.
34 A. Botan, B. Rotenberg, V. Marry, P. Turq and B. Noetinger, *J. Phys. Chem. C*, 2010, **114**, 14962-14969.
35 G. M. Bowers, D. W. Hoyt, S. D. Burton, B. O. Ferguson, T. Varga and R. J. Kirkpatrick, *J. Phys. Chem. C*, 2014, **118**, 3564-3573.
36 J. Breu, W. Seidl and A. Stoll, *Z. Anorg. Allg. Chem.*, 2003, **629**, 503-515.
37 J. Fripiat, *Clays Clay Miner.*, 1974, **22**, 23-30.
38 P. Giesting, S. Guggenheim, A. F. Koster van Groos and A. Busch, *Int. J. Greenh. Gas Con.*, 2012, **8**, 73-81.
39 P. Giesting, S. Guggenheim, A. F. Koster van Groos and A. Busch, *Environ. Sci. Technol.*, 2012, **46**, 5623-5630.
40 D. W. Hoyt, R. V. F. Turcu, J. A. Sears, K. M. Rosso, S. D. Burton, A. R. Felmy and J. Z. Hu, *J. Magn. Reson.*, 2011, **212**, 378-385.
41 E. S. Ilton, H. T. Schaef, O. Qafoku, K. M. Rosso and A. R. Felmy, *Environ. Sci. Technol.*, 2012, **46**, 4241-4248.
42 M. Krishnan, M. Saharay and R. J. Kirkpatrick, *J. Phys. Chem. C*, 2013, **117**, 20592-20609.
43 J. S. Loring, H. T. Schaef, R. V. Turcu, C. J. Thompson, Q. R. Miller, P. F. Martin, J. Hu, D. W. Hoyt, O. Qafoku and E. S. Ilton, *Langmuir*, 2012, **28**, 7125-7128.
44 H. T. Schaef, E. S. Ilton, O. Qafoku, P. F. Martin, A. R. Felmy and K. M. Rosso, *Int. J. Greenh. Gas Con.*, 2012, **6**, 220-229.
45 L. J. Criscenti and R. T. Cygan, *Environ. Sci. Technol.*, 2013, **47**, 87-94.
46 G. M. Bowers, D. L. Bish and R. J. Kirkpatrick, *J. Phys. Chem. C*, 2008, **112**, 6430-6438.
47 G. M. Bowers, J. W. Singer, D. L. Bish and R. J. Kirkpatrick, *J. Phys. Chem. C*, 2011, **115**, 23395-23407.
48 C. A. Weiss Jr, R. J. Kirkpatrick and S. P. Altaner, *Geochim. Cosmochim. Acta*, 1990, **54**, 1655-1669.
49 C. P. Morrow, A. Ö. Yazaydin, M. Krishnan, G. M. Bowers, A. G. Kalinichev and R. J. Kirkpatrick, *J. Phys. Chem. C*, 2013, **117**, 5172-5187.
50 G. Davies, A. Fataftah, A. Cherkasskiy, E. A. Ghabbour, A. Radwan, S. A. Jansen, S. Kolla, M. D. Paciolla, L. T. Sein, A. F. A. C. E. A. G. A. R. S. A. J. S. K. M. D. P. L. T. S. J. W. B. M. B. J. B. B. Xing, W. Buermann, M. Balasubramanian, J. Budnick and B. Xing, *J. Chem. Soc., Dalton Trans.*, 1997, 4047-4060.
51 S. A. Jansen, M. Malaty, S. Nwabara, E. Johnson, E. Ghabbour, G. Davies and J. M. Varnum, *Mater. Sci. Eng., C*, 1996, **4**, 175-179.
52 L. T. Sein, J. M. Varnum and S. A. Jansen, *Environ. Sci. Technol.*, 1998, **33**, 546-552.
53 H. J. C. Berendsen, J. P. M. Postma, W. F. van Gunsteren and J. Hermans, in *Intermolecular Forces*, ed. B. Pullman, Springer Netherlands, 1981, vol. 14, ch. 21, pp. 331-342.
54 R. T. Cygan, J.-J. Liang and A. G. Kalinichev, *J. Phys. Chem. B*, 2004, **108**, 1255-1266.
55 P. Dauber-Osguthorpe, V. A. Roberts, D. J. Osguthorpe, J. Wolff, M. Genest and A. T. Hagler, *Proteins* 1988, **4**, 31-47.
56 T. A. Halgren, *J. Am. Chem. Soc.*, 1992, **114**, 7827-7843.
57 J. A. Greathouse, D. B. Hart, G. M. Bowers, R. J. Kirkpatrick and R. T. Cygan, 2015, DOI: 10.1021/acs.jpcc.5b03314.
58 L. Martínez, R. Andrade, E. G. Birgin and J. M. Martínez, *J. Comput. Chem.*, 2009, **30**, 2157-2164.
59 I. T. Todorov, W. Smith, K. Trachenko and M. T. Dove, *J. Mater. Chem.*, 2006, **16**, 1911-1918.
60 S. Melchionna, G. Ciccotti and B. Lee Holian, *Mol. Phys.*, 1993, **78**, 533-544.
61 G. J. Martyna, D. J. Tobias and M. L. Klein, *J. Chem. Phys.*, 1994, **101**, 4177-4189.
62 G. M. Bowers, M. C. Davis, R. Ravella, S. Komarneni and K. T. Mueller, *Appl. Magn. Reson.*, 2007, **32**, 595-612.